Supplemental Figure 1

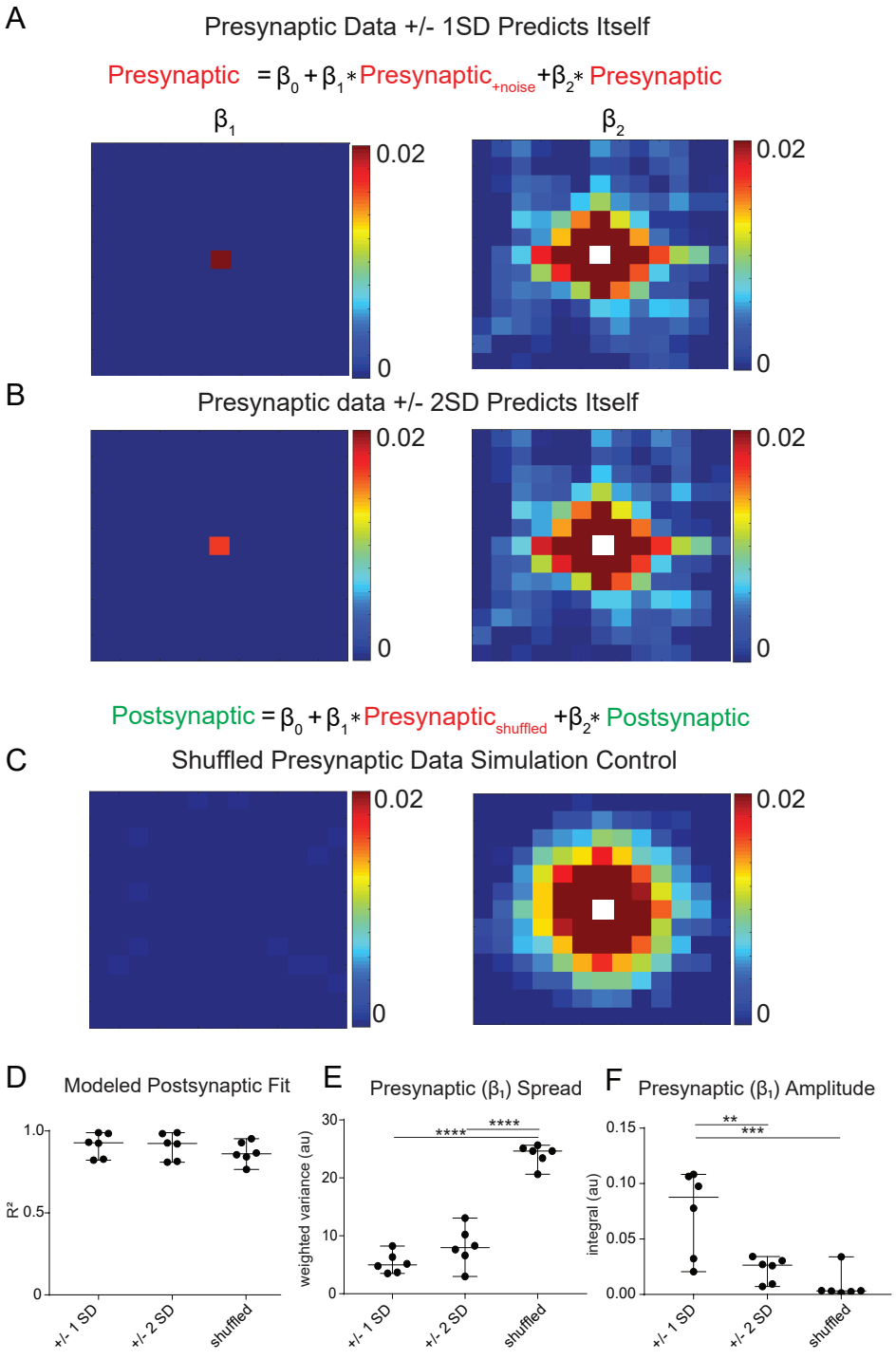

Supplemental Figure 1: Simulation Data; Related to Figure 2

(**A**). To test the regression analysis, we used the presynaptic data set (as in Figure 2), with the addition of +/- 1 standard deviations of noise, to predict itself. This should result in a high-quality prediction, but for the addition of the noise. As expected, the resulting regression analysis indicates a very strong and central presynaptic influence (β_1 coefficient). The surround influence (β_2 coefficient) is similar to before. The data used for this analysis is the original stage 2 retina-to-SC data, with noise added.

(**B**). Same as in (**A**), but now with +/- 2 standard deviations of noise added to the presynaptic data. As expected, the resulting regression analysis shows a highly localized, but smaller presynaptic influence (β1 coefficient), due to the additional noise added.

(**C**). To further test the regression analysis, we randomly shuffled the presynaptic data frames and used them to predict the originally ordered postsynaptic movie. As expected, the resulting regression analysis indicates very low presynaptic predictive influence (β_1 coefficient – left panel), and a very strong postsynaptic (surround) influence (β_2 coefficient – right panel).

(**D-F**). Summary quantification of the test regression analyses. R-squared was high in all cases (**D**), the presynaptic spread (weighted variance) was much larger for the shuffled data (**E**), and the presynaptic amplitude (integral) was largest for the weakly noisy data, and very weak for the shuffled data (**F**) across all 6 mouse data sets. The differences were statistically significant as determined by one-way ANOVA, $F=14.33$, $p=0.0003$ (**D**), $F=76.57$, $p<0.0001$ (**E**), $F=19.51$, $p<0.0001$ (**F**). P statistics from multiple comparisons with Tukey's correction indicated on the graph.

Supplemental Figure 2

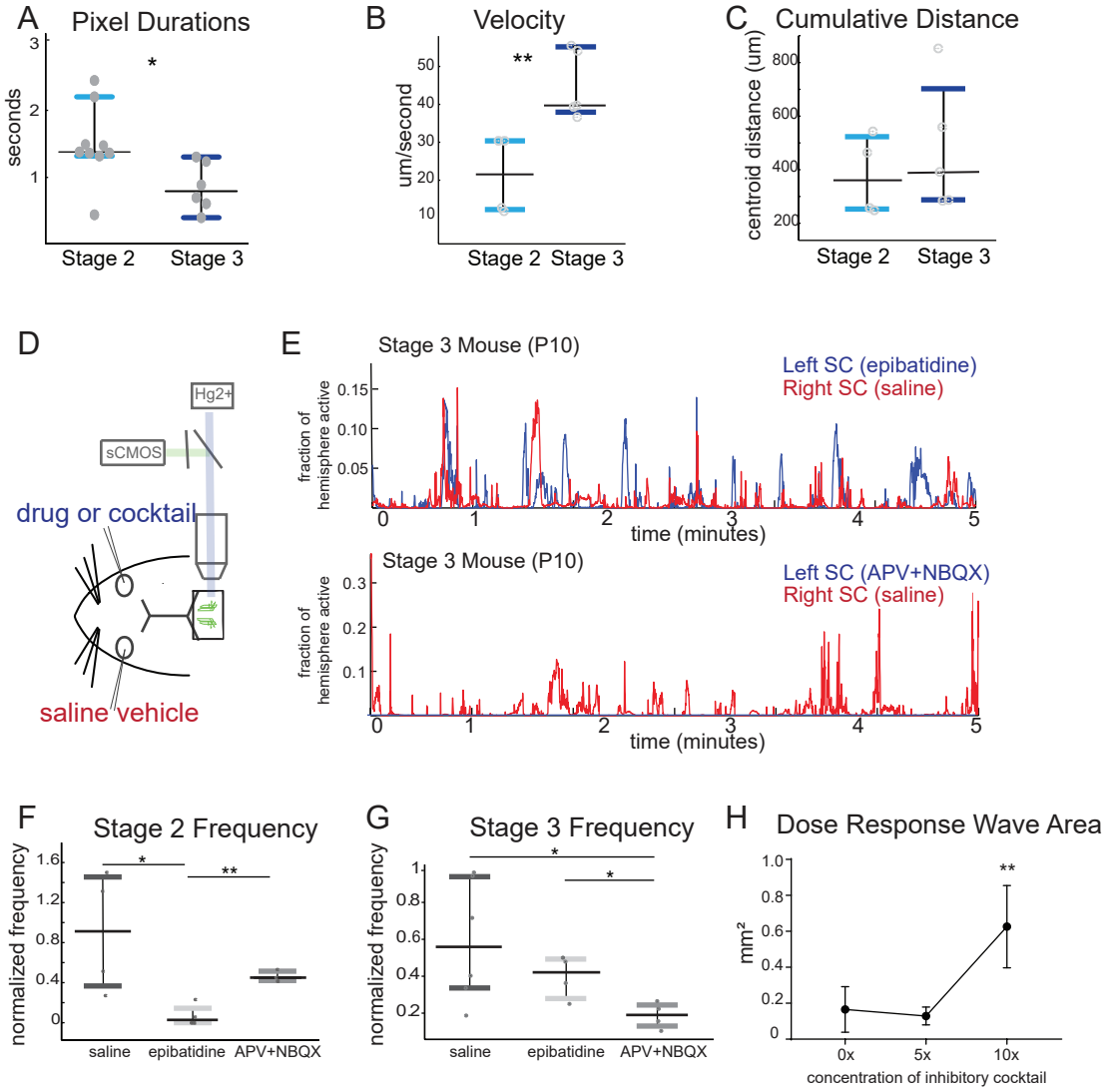

Supplemental Figure 2: Additional Wave Properties; Related to Figure 3
(**A-C**). Summary statistics for additional properties of stage 2 and stage 3 waves, including duration of wave activity measured by pixel (**A**), wave velocity (**B**) and distance of wave propagation across the superior colliculus (**C**).

(**D**) Experimental set up for applying pharmacological agents to the retina. Retinal ganglion cell axons in the SC are imaged after injecting a saline control in one eye, and a pharmacological agent (drug) in the other eye.

(**E**) Example of the effect of nAChR function blocking agent, 10 mM epibatidine (top), and glutamate receptor anatgonists, 1 mM AP5 and 200 µM NBQX (bottom), on stage 3 waves. APV + NBQX eliminated stage 3 wave activity, but epibatidine does not, consistent with a glutamatergic (but not cholinergic) origin of stage 3 waves.

(**F-G**). Summary quantification of the effect of pharmacological manipulations on stage 2 (**F**) and stage 3 (**G**). waves. Normalization was done to pre-injection period; saline controls were within-animal controls. The frequency of stage 2 waves was significantly reduced by epibatidine, but not APV + NBQX (**C**), while the frequency of stage 3 waves was significantly reduced by APV + NBQX but not epibatidine (**D**).

(**H**). A lower concentration of the inhibitory cocktail, 5 times (250 µM TPMPA, 25 µM gabazine , and 2.5 uM strychnine) that used in previous *in vitro* studies (Akrouh and Kerschensteiner, 2013), did not have a demonstrable effect, thus the 10X (500 µM TPMPA, 50 µM gabazine , and 5 uM strychnine) concentration described above was used for the remainder of all experiments.

Supplemental Figure 3

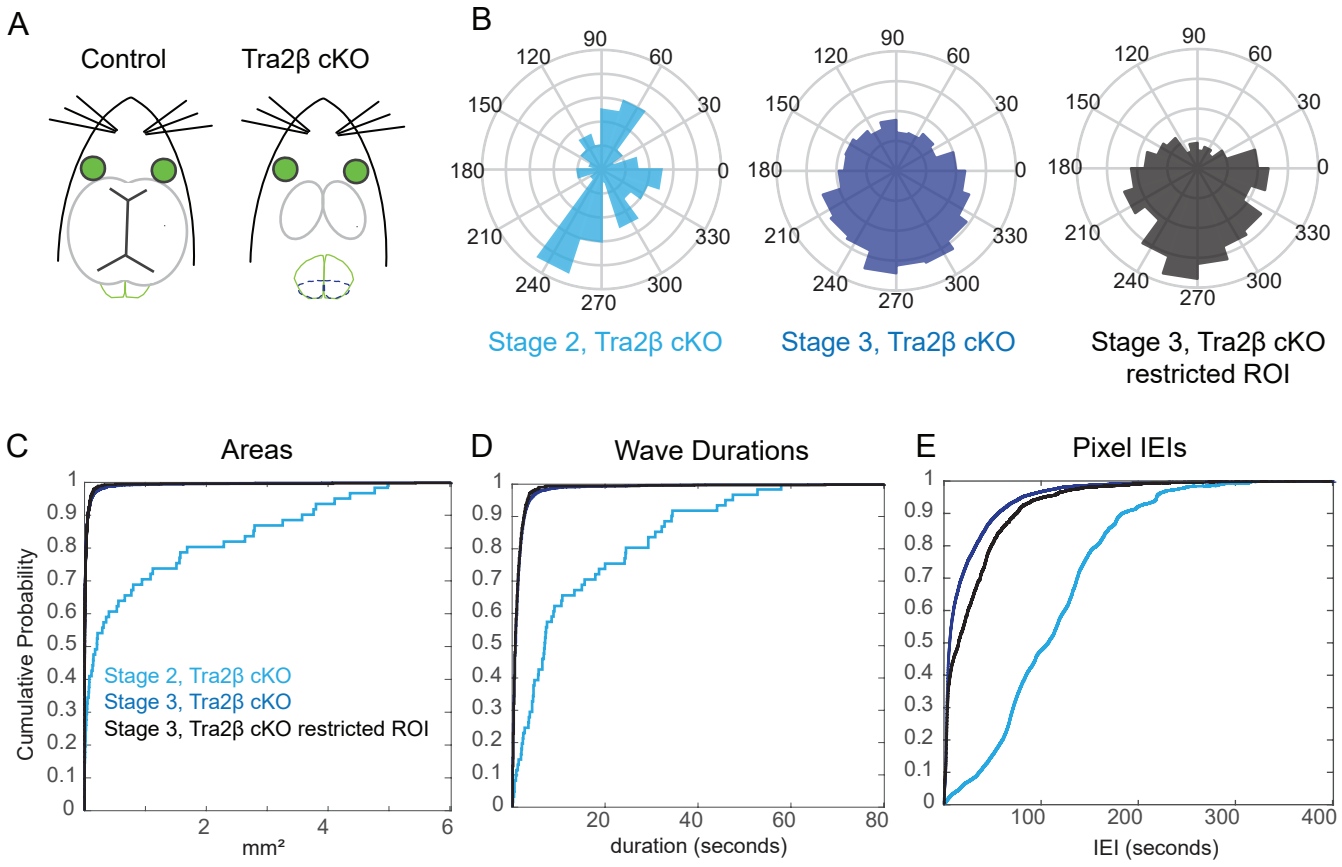

Supplemental Figure 3: Stage 3 directionality differences persist with access to entire retinotopic area; Related to Figure 3

(**A**). Cartoon depiction of a control mouse (left - Control), in which the colliculus is progressively obscured through developmental overgrowth by the cortex and cortexless (right - Tra2β cKO) mice (Shanks et al., 2016), in which it is possible to visualize the entire dorsal surface of the colliculus.

(**B**). Wave directionality in cortexless mice for stage 2 (n=4), stage 3 (n=3), and stage 3 with analysis restricted to caudal section ('restricted ROI'), i.e. the region that is normally visible in controls. Access to the full SC does show more waves moving in the rostral direction, but the vast majority of waves still move in a rostral to caudal direction. Circular variance (CV) of stage 2 = 0.9003, stage 3 CV=0.7908; CV of stage 3 restricted analysis = 0.6694.

(**C-E**). Access to the entire SC does not change measurements of area or wave duration for stage 3 ($p=0.352$ and $p=0.783$, respectively, K-S test), but does have a significantly different inter-event-interval ($p<<0.0001$), suggesting that there is higher frequency of activity rostral to our usually imaged portion and closer to the center for the visual field. Light blue is stage 3 Controls, dark blue is stage 3 Tra2β cKO, black is stage 3 Tra2β cKO with analysis restricted to the comparable caudal section of the SC as in control mice ('restricted ROI').

Supplemental Figure 4

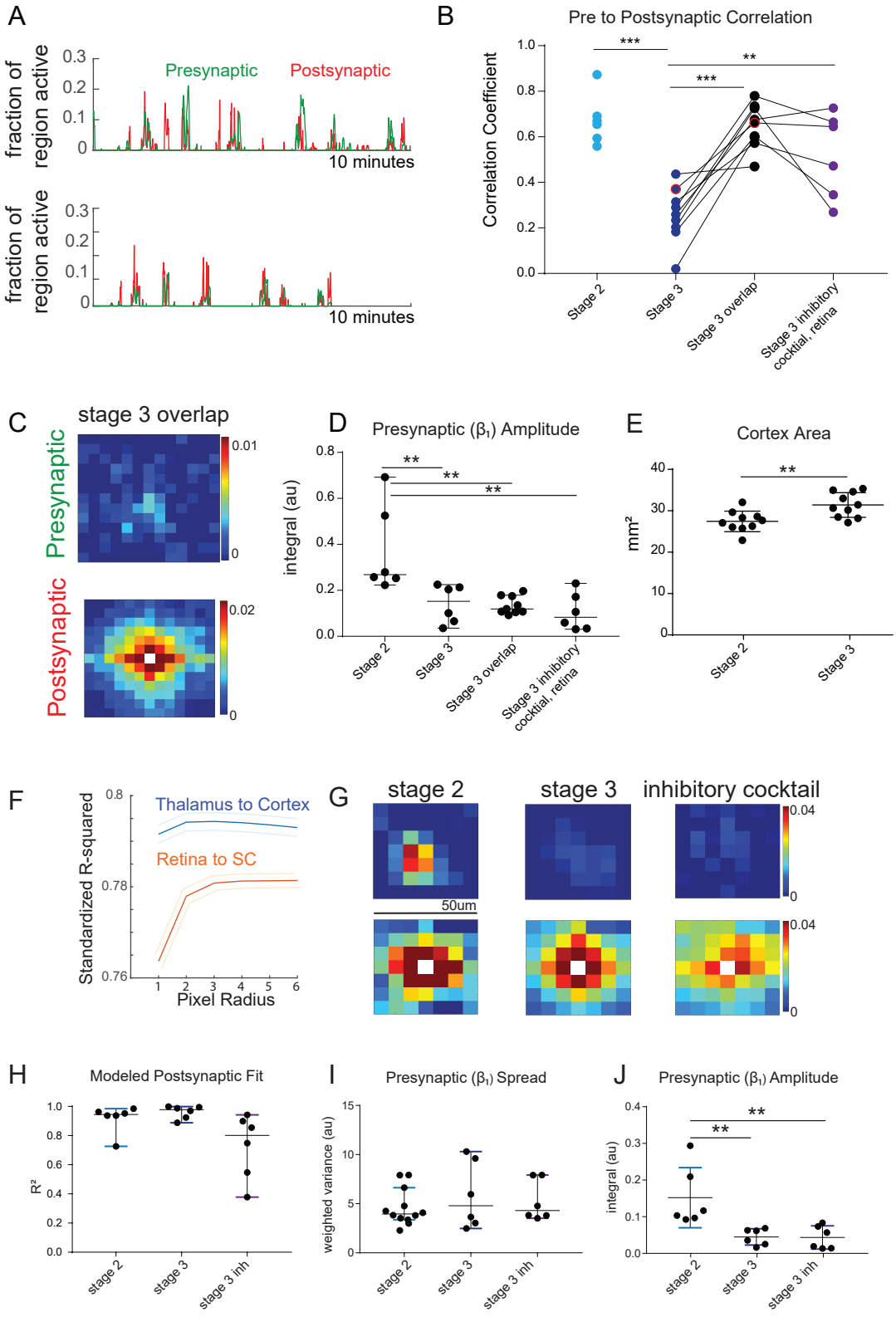

Supplemental Figure 4: Additional Regression Analyses; Related to Figure 4
(**A**). Example of presynaptic thalamic activity (green) and postsynaptic cortical activity (red) traces for a mouse during stage 3 waves (top) and after removing times when there was a mismatch between presynaptic and postsynaptic activity (bottom).

(**B**). Summary quantification of presynaptic to postsynaptic correlation (data from **Figure 4D)** with the addition of the new correlation measurements (Stage 3 overlap) after removing frames in which presynaptic and postsynaptic activity is mismatched. As expected, confining the correlation analysis to frames when the presynaptic and postsynaptic data overlap increases the correlation coefficient.

(**C**). Regression analysis, as in **Figure 4F**, but confined to frames with high correlation between presynaptic (thalamic) and postsynaptic (cortical) activity, as in (**A**).

(**D**). Summary quantification of the presynaptic (β_1) amplitude with analysis confined to stage 3 overlap frames in comparison to all the frames (as in **Figure 4F** for comparison). Confining the analysis to overlap frames does not increase the presynaptic (β_1) amplitude. This confirms that the decrease in the functional influence (presynaptic (β_1) amplitude) of the thalamus on the cortex is not specifically due to a decrease in the correlation of presynaptic thalamic activity to postsynaptic cortical activity in stage 3 relative to stage 2.

(**E**). Cortex growth between stage 2 and stage 3. Cortex area is approximately 14% larger between stage 2 (27.44 ± 0.7832, n=10) and stage 3 (31.4 ± 0.9443, n=10, $p<0.01$).

(**F**). Leave-one-out cross validation comparisons (n= 6 animals) indicate a smaller surrounding region (Pixel radius 3) is best to describe the thalamic to cortical transfer, whereas even larger pixel radii are gradually better for the retina to SC transfer as measured through the regression analysis. This is consistent with a smaller, more focal effect of the thalamus on the cortex than the retina on the SC.

(**G**). Top panels show the presynaptic (β_1) coefficients that represent the contribution of nearby presynaptic activity to each postsynaptic pixel in the thalamus to cortex data with a pixel radius of 3 for the transfer function. The bottom panels display the contribution of surrounding postsynaptic activity (β_2 coefficients) for pixel radius 3.

(**H**). The regression model fit (R-squared) is high for stage 2, stage 3 and stage 3 with inhibitory cocktail applied to the retina using a pixel radius of 3 for the kernel. This i similar to the full kernel model (Figure 4).

(**I**). The spatial spread (weighted variance, see Methods) of the influence of the presynaptic thalamic activity on postsynaptic cortical activity (β_1 coefficient spread) is small and similar for stage 2, stage 3 and stage 3 with inhibitory antagonists when using a pixel radius of 3 for the kernel. This is similar to the full kernel model (Figure 4).

(**J**). The strength of the influence of presynaptic thalamic activity on postsynaptic cortical activity (β_1 coefficient amplitude) is significantly smaller in stage 3 than in stage 2, and similarly small in stage 3 with inhibitory antagonist applied to the retina when using the pixel radius of 3 kernel. This is similar to the relationships observed using larger kernels as shown in Figure 4.

Supplemental Figure 5

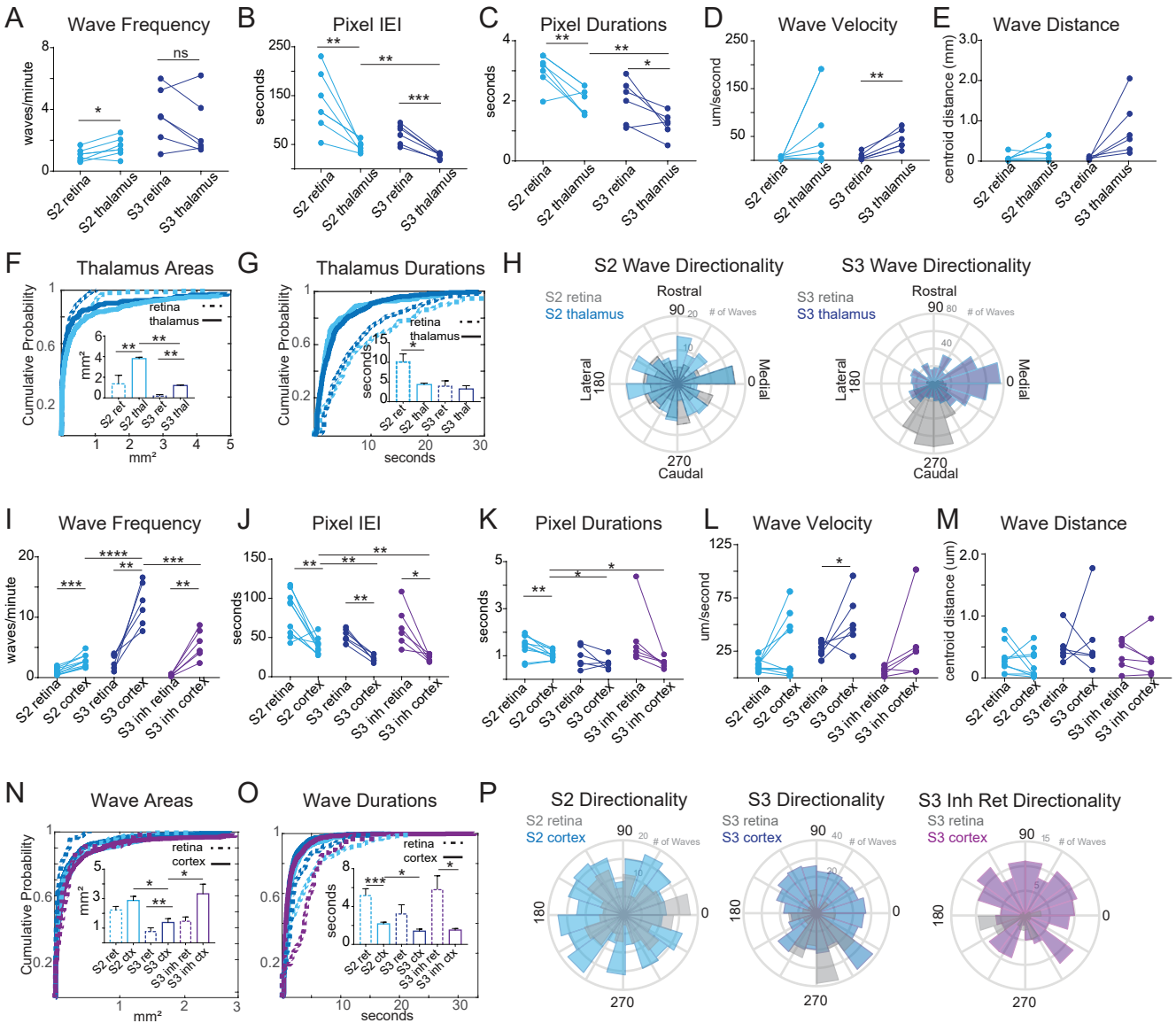

Supplemental Figure 5: Thalamus and Cortex Wave Properties; Related to Figure 5
(**A-G**). Wave properties for thalamic and retinal waves during stage 2 (n=6 hemispheres) and stage 3 (n=6 hemispheres). Asterisks indicate properties that were significantly different from one or more groups within that category of properties. Significance was measured using one-way ANOVA using Tukey's correction for multiple comparisons. Wave areas were smaller in stage 3 compared to stage 2 ($p = 0.0327$, K-S test), and durations were briefer during stage 3 ($p = 0.0449$, K-S test).

(**H**). Wave directionality plots for thalamic waves and retinal waves; stage 3 waves are comparably directional in the thalamus as in the retinal axons (CV of stage 2 thalamus = 0.9356, simultaneous stage 2 retina CV=0.9020; CV of stage 3 thalamus = 0.7783, stage 3 retina CV = 0.2959; $p=0.0418$ thalamus for individual mouse CV, $p=0.0003$ for simultaneous retinal CVs).

(**I-O**). Wave properties for retinal and cortical waves during stage 2 (n=9 hemispheres), stage 3 (n=6 hemispheres), and stage 3 after inhibitory blocker (n=6 hemispheres). Cortical waves where imaged by using Rx-Cre x floxed GCaMP6f mice. Asterisks indicate properties that were significantly different from one or more groups within that category of properties. Significance was measured using one-way ANOVA using Tukey's correction for multiple comparisons. Wave areas were smaller in stage 3 compared to stage 2 ($p < 0.0001$, K-S test), and durations were briefer during stage 3 ($p < 0.00001$, K-S test). Interestingly, stage 2 areas were not significantly different from wave areas in stage 3 after retinal inhibitory blocker ($p = 0.98$, K-S test), and wave durations were not significantly different between stage 3 and stage 3 after retinal inhibitory block ($p = 0.313$, K-S test).

(**P**) Wave directionality plots for retinal waves and cortical waves. CV of stage 2 cortex = 0.8918, simultaneous stage 2 retina CV=0.8820; CV of stage 3 cortex = 0.9617, stage 3 retina CV = 0.5799; CV of stage 3 cortex after retinal inhibition is blocked = 0.8958, stage 3 retina after inhibitory blocker cocktail CV = 0.5542; for stage 3 retinal directionality, $p<0.01$ when compared to stage 2 retina, and cortical directionality in any condition. Significance was measured using one-way ANOVA on individual mouse CV values and Tukey's correction for multiple comparisons.